

\mathcal{PT} -Symmetry breaking in quantum spin chains with exceptional non-Hermiticities

Jacob Muldoon and Yogesh N. Joglekar

Department of Physics, Indiana University-Purdue University Indianapolis (IUPUI), Indianapolis, Indiana 46202

Since the realization of quantum systems described by non-Hermitian Hamiltonians with parity-time (\mathcal{PT}) symmetry, interest in non-Hermitian, quantum many-body models has steadily grown. Most studies to-date map to traditional quantum spin models with a non-Hermiticity that arises from making the model parameters complex or purely imaginary. Here, we present a new class of models with non-Hermiticity generated by splitting a Hermitian term into two Jordan-normal form parts. We present exact diagonalization results for the \mathcal{PT} -threshold in such models, and provide an analytical approach for understanding the numerical results. Surprisingly, with non-Hermitian potentials confined to two or even a single site, we find a robust \mathcal{PT} threshold that is insensitive to the size of the quantum spin chain. Our results provide a pathway to experimentally feasible non-Hermitian quantum spin chains where the confluence of many-body effects and non-Hermiticity effects can be observed.

I. INTRODUCTION

Since the seminal discovery of Bender and co-workers 25 years ago [1], the field of non-Hermitian systems has dramatically flourished. Research initially focused on continuum, non-relativistic Schrödinger equations with complex (often, purely imaginary) potentials that were invariant under combined operations of parity and time-reversal, i.e. $V(x) = V^*(-x)$ [2–4]. Such \mathcal{PT} -symmetric Hamiltonians showed purely real spectra at small non-Hermiticity, going over to complex-conjugate spectra at large non-Hermiticity [5, 6]. Experiments in wave systems (optics [7–9], acoustics [10], and the like [11, 12] with balanced, spatially separated gain and loss, provided a simple physical interpretation for \mathcal{PT} -symmetric Hamiltonians as effective models for open systems [13, 14]. From this vantage point, the \mathcal{PT} -symmetry breaking transition marks the concomitant emergence of amplifying and decaying modes in an open system. Thus, in the classical domain, \mathcal{PT} -symmetric Hamiltonians are often modeled with purely anti-Hermitian potentials that signify local amplification or absorption. Over the years, these ideas have been generalized to time-periodic models [15–17], non-Markovian models [18, 19], and synthetic degrees of freedom [20, 21], all in the classical domain.

In the quantum domain, creation of balanced gain and loss potentials is precluded by thermal fluctuations associated with the dissipation [22], and even at zero temperature, the quantum noise associated with linear amplifiers [23, 24]. Instead, the coherent, non-unitary dynamics generated by \mathcal{PT} -symmetric Hamiltonians is simulated by mode-selective losses [25, 26], Hamiltonian dilation [27], or unitary dilation [28] methods. Most recently, it was realized that a Lindbladian, minimal quantum system [29–31], when post-selected on trajectories that do not undergo quantum jumps [32, 33], is described by a non-Hermitian, \mathcal{PT} -symmetric Hamiltonian with state-dependent, trace-preserving non-linearity [34]. This technique has enabled the exploration of non-Hermitian Hamiltonians in quantum, two-level systems [35–37]. With this approach, an exponentially decaying no-jump probability caps the duration of the coherent, non-

unitary dynamics, and post-selection gives rise to anti-Hermitian potentials. Therefore, theoretical studies of non-Hermitian, quantum many-body models have typically commenced by changing parameter(s) in their Hermitian counterparts from real to complex [38–46].

Here we present a new set of models with non-Hermiticity created by splitting a Hermitian potential into two, Jordan-form terms and then spatially separating them. For example, in a transverse field quantum Ising model, this means $\gamma\sigma_m^x \rightarrow \gamma(\sigma_{m-n}^+ + \sigma_{m+n}^-)$ where σ_m^α represents the relevant Pauli operator on site m . Note that $\sigma^\pm \equiv (\sigma^x \pm i\sigma^y)/2$ are rank-1, Jordan normal form matrices; they represent single-qubit Hamiltonian at an exceptional point. In quantum spin systems with finite number of levels, the mapping between raising/lowering operators σ^\pm and gain/loss is ambiguous due to the presence of a ceiling in the spectrum. On the contrary, in bosonic models such as two coupled oscillators, this splitting procedure will generate non-Hermitian gain/loss potentials such as $\gamma(a_1^\dagger + a_2)$. We emphasize that the operators a_1^\dagger, a_2 are terms in the Hamiltonian, not dissipators routinely used in Lindblad dynamics to model spontaneous emission and absorption; the latter give rise to anti-Hermitian potentials [47].

In this paper, we investigate the \mathcal{PT} -symmetry breaking threshold in transverse field Ising models with finite number of spins N and its dependence on parameters using exact diagonalization method. Other traditional techniques such as perturbation theory or tensor networks are ideal for probing a small, ground-state-approximate subspace of the exponentially-large Hilbert space. Determining \mathcal{PT} -breaking threshold—where the Hamiltonian first develops complex-conjugate eigenvalues—requires knowledge of the entire spectrum, since the states that develop complex eigenvalues are typically not at the bottom (or the top) of the band [48].

The plan of the paper is as follows. In Sec. II we introduce the canonical quantum Ising chain and its non-Hermitian variations. The non-Hermitian variations on it consist of perturbations on one or two sites. In addition to the \mathcal{PT} -threshold, we also present the flow of eigen-

values across the \mathcal{PT} -symmetry breaking transition. In Sec. III we present a simple analytical approach that explains the surprisingly robust \mathcal{PT} threshold results from Sec. II. We conclude the paper in Sec. IV with higher-spin generalizations, brief feasibility analysis, and summary. The \mathcal{PT} -threshold results are valid for chains with $N > 2$ where the bulk-vs-edge sites and periodic-vs-open boundary conditions are unambiguously defined, but do not depend on N .

II. NON-HERMITIAN QUANTUM ISING MODELS

The canonical quantum Ising model with N sites is described by the Hamiltonian

$$H_0(J, h_z) = -\frac{J}{4} \sum_{i=1} \sigma_i^x \sigma_{i+1}^x - \frac{h_z}{2} \sum_{i=1} \sigma_i^z \quad (1)$$

where $J > 0$ is the ferromagnetic coupling between adjacent spins, the uniform transverse field is along the z -axis, and the boundary term $\sigma_N^x \sigma_1^x$ is included when periodic-boundary conditions are required [49, 50]. This exactly solvable model undergoes a quantum phase transition from a spontaneously-broken \mathbb{Z}_2 -symmetry phase to a paramagnetic phase with short-range correlations as the transverse field strength crosses $h_z = J/2$ [51, 52]. In this section, we investigate its varied non-Hermitian extensions.

A. Two-site Perturbations with Hermitian or anti-Hermitian limit ($h_z = 0$)

Consider the non-Hermitian extension

$$H_{\text{eff}}(J, h_z|\gamma) = H_0(J, h_z) + \Gamma_{pq}^+(\gamma), \quad (2)$$

$$\Gamma_{pq}^+ = \gamma(\sigma_p^+ + \sigma_q^-) \neq \Gamma_{pq}^{+\dagger}, \quad (3)$$

where $\gamma > 0$ is the strength of the exceptional perturbations σ^\pm , and $1 \leq p, q \leq N$ denote their locations along the chain. When $p = q$, the perturbation Eq.(3) is trivially Hermitian and the system has no threshold. Since H_{eff} has real entries, its characteristic polynomial has real coefficients and its eigenvalues are real or complex conjugates [53].

Figure 1 summarizes the \mathcal{PT} -threshold phase diagram of such quantum spin chain in the absence of transverse field. It involves calculating the spectrum of $H_{\text{eff}}(J, 0|\gamma)$ by exact diagonalization, and then recursively increasing the strength of Γ^+ until complex-conjugate eigenvalues emerge at the threshold γ_{PT} . Figure 1(a) shows the dimensionless threshold γ_{PT}/J for an $N = 7$ open chain as a function of (p, q) , but the results remain the same for any chain size $N > 2$. Ignoring the trivial Hermitian case ($p = q$; black, filled circles), the threshold results can be

grouped into three categories:

Adjacent sites ($|p - q| = 1$) : $\gamma_{\text{PT}} = 0$ (red circles); (4)

Edge sites ($|p - q| > 1$) : $\gamma_{\text{PT}} = J/4$ (blue circles); (5)

Bulk sites ($|p - q| > 1$) : $\gamma_{\text{PT}} = J/2$ (green circles). (6)

When periodic boundary conditions are imposed on Eq.(1), the "edge sites" category, Eq.(5), disappears; the threshold is zero when the perturbations σ^\pm are on adjacent sites and $\gamma_{\text{PT}} = J/2$ when they do not share a bond. These results are robust with respect to the number of spins ($N > 2$), (open or periodic) boundary conditions, or the distance $|p - q| \geq 2$ and the locations of the two sites along the chain. This surprising nonzero threshold implies that the \mathcal{P} -operator is not the spatial reflection, $k \leftrightarrow N + 1 - k$. Indeed, since the Hamiltonian $H_{\text{eff}}(J, h_z|\gamma)$ is purely real, its antilinear symmetry can be chosen as $\mathcal{P} = \mathbb{1}_N$ and $\mathcal{T} = *$ (complex conjugation).

To understand the mechanism of \mathcal{PT} -symmetry breaking under exceptional perturbations, we show the flow of eigenvalues $\text{Re}(E)$ (blue lines) and $\text{Im}(E)$ (red lines) as a function of γ/J in Figs. 1(b)-(f). Since the eigenvalues occur in complex-conjugate pairs, it is sufficient to plot $\text{Im}(E) > 0$. When the potentials are maximally separated, $(p, q) = (1, N)$, starting from N bands with varying degeneracies, a set of central bands undergo level attraction and develop imaginary parts at $\gamma = J/4$, Fig. 1(b). The ground state (or its particle-hole symmetric counterpart) does not participate in \mathcal{PT} -symmetry breaking. Figure 1(c), with $(p, q) = (6, 4)$ shows that for bulk, non-adjacent sites, again, \mathcal{PT} -symmetry breaks with multitude of bands across the energy-level spectrum at $\gamma = J/2$. The trivial case of a Hermitian perturbation, $p = 1 = q$ shows expected linear level-splitting, Fig. 1(d). When the perturbation sites share a bond, $(p, q) = (2, 1)$ linearly increasing $\text{Im}(E)$ signal the zero threshold, Fig 1(e). We note that the bands developing complex eigenvalues are neither particle-hole symmetric nor at the bottom or the top. Lastly, when the edge perturbation sites are not maximally separated, $(p, q) = (6, 1)$, the flow of eigenvalues is different, Fig. 1(f), from the results in Fig. 1(a).

Next, we replace the Γ_{pq}^+ potential by

$$\Gamma_{pq}^- = \gamma(\sigma_p^+ - \sigma_q^-) \quad (7)$$

which reduces to an anti-Hermitian term $\Gamma_{pp}^- = i\gamma\sigma_y$ when $p = q$. When $p \neq q$, the \mathcal{PT} -threshold $\gamma_{\text{PT}}(p, q) = \gamma_{\text{PT}}(q, p)$ is given by Eqs.(4)-(6). When $p = q$, the resulting threshold $\gamma_{\text{PT}}(p, p) = 0$ for a bulk site, whereas $\gamma_{\text{PT}} = J/4$ for an edge site. Once again, these results are robust against the number of spins $N > 2$, the distance $|p - q| > 1$ between the perturbations, and nature of boundary conditions. Here, too, since Eq.(7) has purely real entries, $\mathcal{PT} = \mathbb{1}_N*$ gives the corresponding antilinear symmetry.

The simple expressions for the \mathcal{PT} -threshold, Eqs.(4)-(6), hint at an analytical solution. At this point, it is

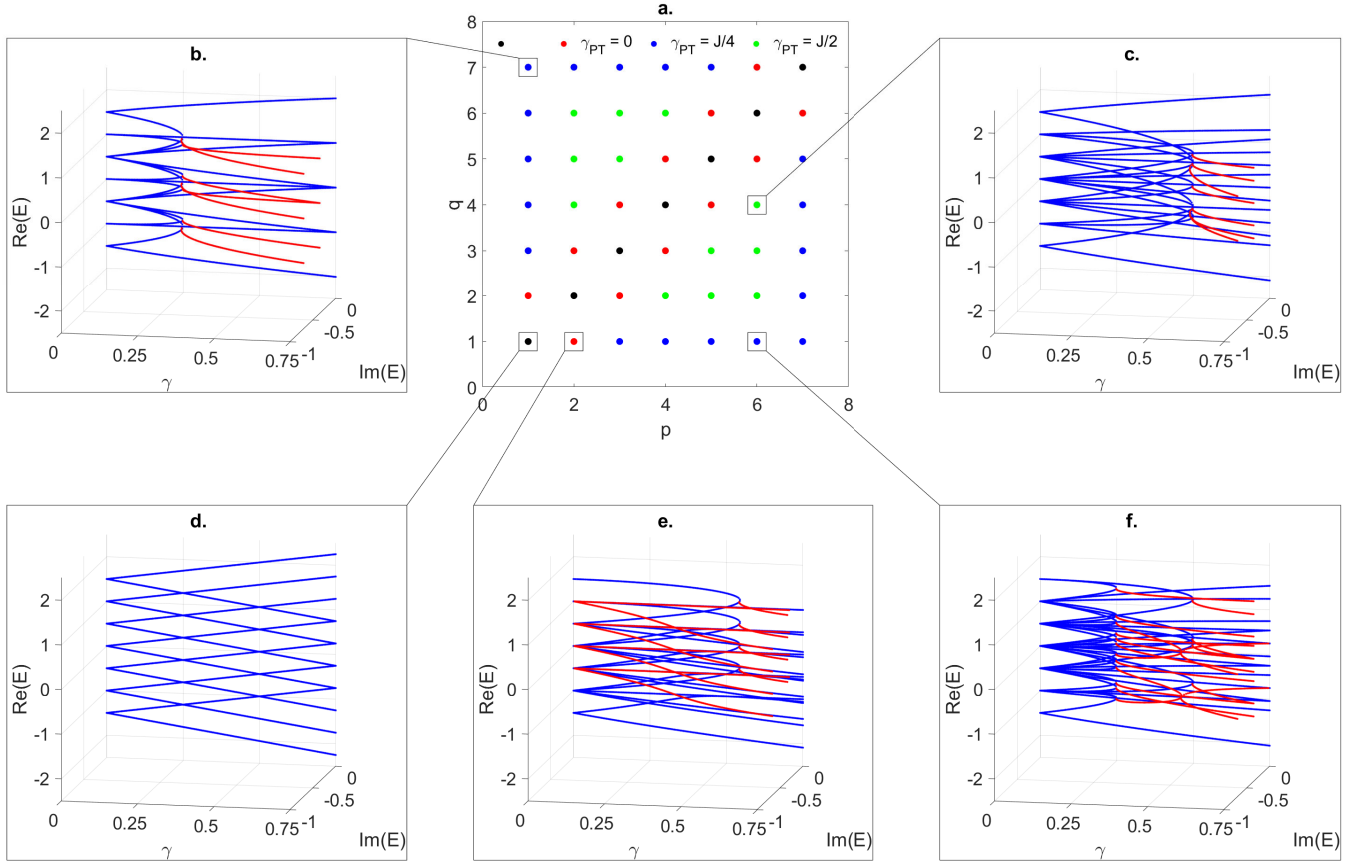


Figure 1. \mathcal{PT} -breaking threshold for a 7-spins chain with $h_z = 0$ and non-Hermiticity $\Gamma_{p,q}^+$, Eq.(3). (a) Apart from the Hermitian case at $p = q$ (black circles), threshold takes three possible values: zero for adjacent sites (red circles); $\gamma_{PT}(p, q) = J/4$ when at least one site is at the edge (blue circles); and $\gamma_{PT}(p, q) = J/2$ when both sites are in the bulk. (b)-(f) show the flow of eigenvalues $Re(E)(\gamma)$ (blue lines) and $Im(E)(\lambda) > 0$ (red lines) for p, q locations marked in (a). At $\gamma = 0$, the system has 7 particle-hole symmetric bands with varying degeneracies spanning the $2^7 = 128$ eigenvalues; at a finite γ , the particle-hole symmetry is generally broken. Ground-state band typically does not participate in the \mathcal{PT} -symmetry breaking transition. Therefore, variational or perturbative methods that focus on the lowest-lying states cannot be used to determine the \mathcal{PT} -symmetry breaking threshold.

important to recall that the spectrum of the Hamiltonian Eq.(1) is traditionally obtained by using the Jordan-Wigner transformation to map the problem onto non-interaction fermions [51, 52]. Under this mapping, however, the exceptional perturbations σ_p^+, σ_q^- create non-Hermitian, fermionic string operators, thereby rendering such an approach useless.

B. Single-site Perturbations ($h_z = 0$)

Inspired by the repeating structure of bands in Fig. 1, and the finite \mathcal{PT} -threshold obtained in the anti-Hermitian limit of Eq.(7), we now consider the Ising spin chain with a single-site perturbation,

$$\Gamma_p(\gamma_+, \gamma_-) = \gamma_+ \sigma_p^+ + \gamma_- \sigma_p^-, \quad (8)$$

where $\gamma_{\pm} \in \mathbb{R}$ denote the strengths of (exceptional) non-Hermiticities σ_p^{\pm} that act on the spin at site p . Starting with the case $\gamma_- = 0$, the \mathcal{PT} -breaking threshold for the Hamiltonian $H_0 + \Gamma_p(\gamma, 0)$ is given by

$$\gamma_{PT}(p) = \begin{cases} J/4 & \text{Edge case,} \\ J/2 & \text{Bulk case.} \end{cases} \quad (9)$$

Figure 2 shows the evolution of the energy-spectra of an $N = 8$ chain as a function of γ when the sole-perturbation σ^+ is on the edge site (a) and the bulk site, $p = 2$ (b). These results have many features common with the eigenvalue flows in Fig. 1. Specifically, we see that starting with N particle-hole symmetric bands at $\gamma = 0$ that the \mathcal{PT} breaking occurs at a threshold equal to $J/4$ or $J/2$ respectively, but the ground-state eigenvalue does not become complex. Since a unitary basis-change can map $\sigma_y \rightarrow -\sigma_y$ without changing interaction

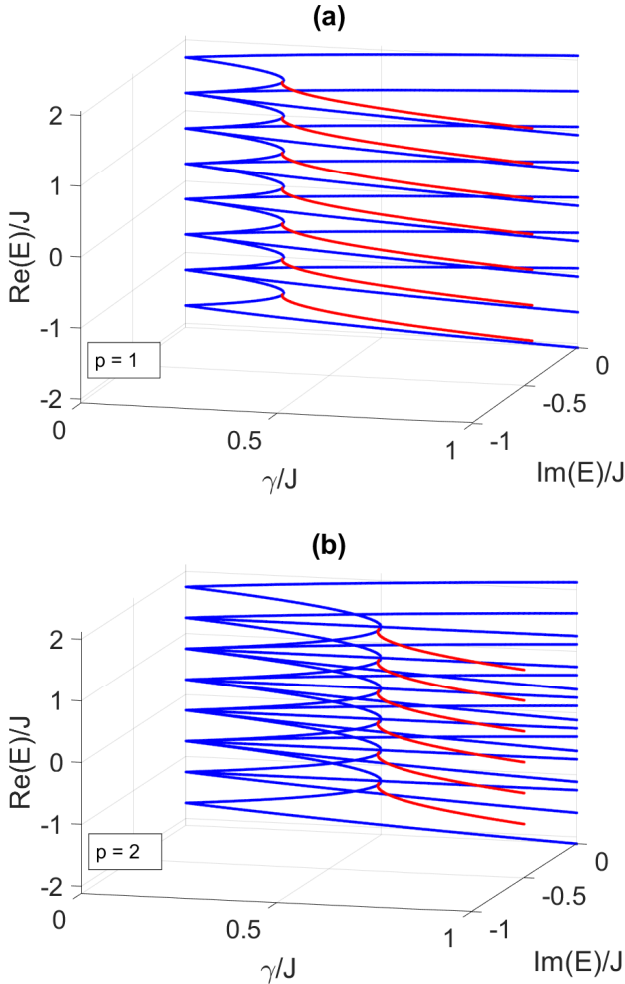


Figure 2. Flow of eigenvalues $\text{Re}(E)(\lambda)$ (blue lines) and $\text{Im}(E)(\lambda)$ (red lines) for an 8-spins chain with potential $\gamma\sigma^+$ on one site. At $\gamma = 0$, the system has 8 particle-hole symmetric bands with varying degeneracies that account for the total $2^8 = 256$ eigenvalues. (a) When the site is at the edge, $\text{Im}(E) > 0$ emerge past the threshold $\gamma_{\text{PT}} = J/4$. (b) For a bulk site, $p = 3$, the complex-conjugate eigenvalues occur past the threshold $\gamma_{\text{PT}} = J/2$.

term in H_0 , Eq.(1), the threshold results for a $\Gamma_p(0, \gamma)$ -perturbation are the same as in Eq.(9).

Lastly, we consider the case where both γ_{\pm} are varied. The non-Hermitian, purely real Hamiltonian is given by

$$H_{\text{eff}} = H_0 + (\gamma_+ + \gamma_-)\sigma_p^x + i(\gamma_+ - \gamma_-)\sigma_p^y. \quad (10)$$

We characterize the \mathcal{PT} phase diagram in the (γ_+, γ_-) plane by plotting the largest imaginary part of the eigenvalues of $H_{\text{eff}}(\gamma_+, \gamma_-)$ obtained via exact diagonalization (Fig. 2). It indicates whether the system is in the \mathcal{PT} -symmetric phase ($\max \text{Im}(E) = 0$; deep blue) or \mathcal{PT} -symmetry broken phase ($\max \text{Im}(E) > 0$; other colors), and quantifies the amplification rate for the \mathcal{PT} -broken eigenstates. Along the diagonal $\gamma_+ = \gamma_-$, H_{eff} is Hermitian and the spectrum is always real. Along the other

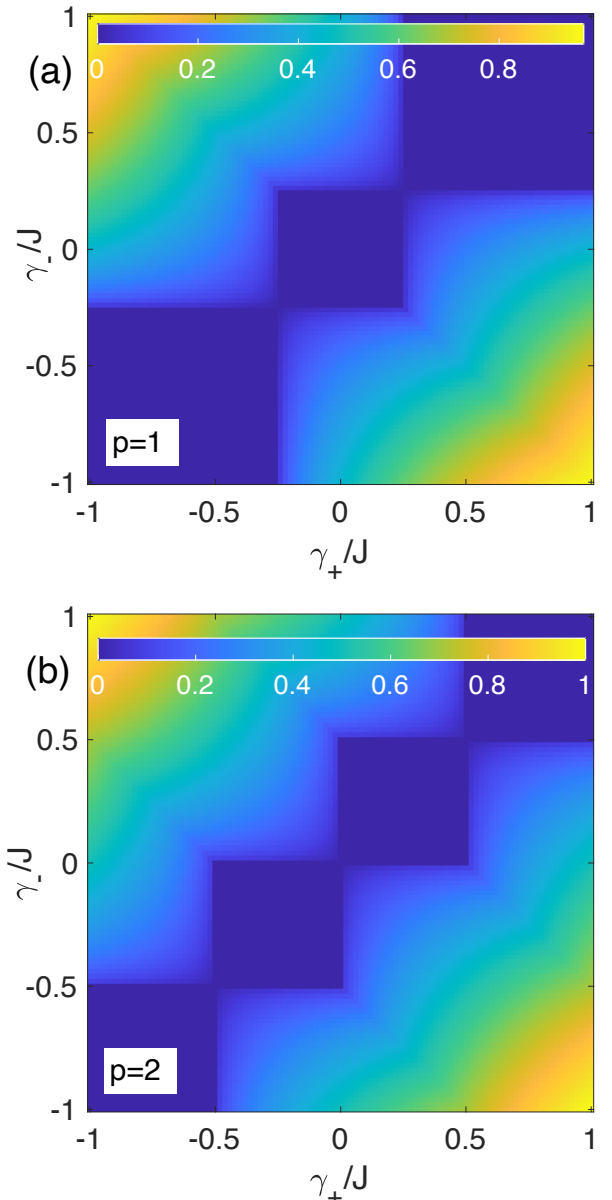


Figure 3. \mathcal{PT} -phase diagram of a 6-spins chain in (γ_+, γ_-) plane. Color denotes maximum imaginary part $\text{Im}(E)/J$ of the eigenvalues of Hamiltonian Eq.(10). Deep blue regions indicate \mathcal{PT} -symmetric phase. (a) When the perturbation site is at the edge ($p = 1$), γ_{PT} is positive along the anti-diagonal. (b) When the site is in the bulk ($p = 2$), the threshold is zero.

diagonal, given by $\gamma_+ + \gamma_- = 0$, the perturbation (8) is anti-Hermitian. In this case, we obtain a positive threshold for the edge case (Fig. 2(a)), while the threshold is zero for the bulk case (Fig. 2(b)), as seen in Sec. II A.

The \mathcal{PT} phase-diagram in Fig. 3 is symmetric under individual reflections across the two diagonals. Since $\text{Im}(E)(\lambda_+, \lambda_-)$ is an even function of the strength of the $i\sigma^y$ term in Eq.(10), reflection symmetry along the main diagonal is expected. Reflection symmetry along

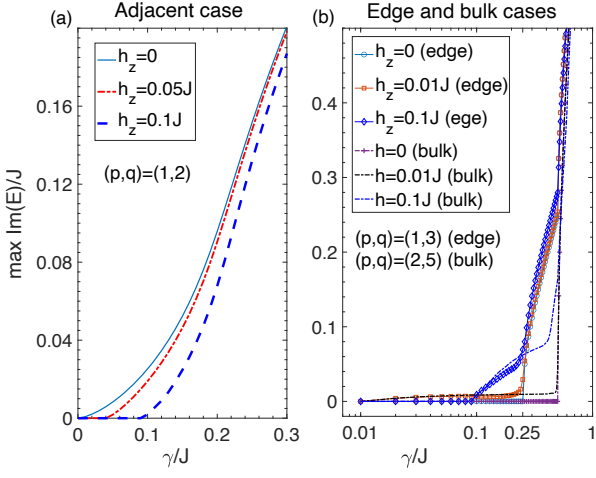


Figure 4. Threshold $\gamma_{\text{PT}}(h_z)$ for Hamiltonian Eq.(2) with $N = 9$ spins. (a) For perturbation Γ_{pq}^+ , adjacent sites with zero threshold develop a finite threshold $\propto |h_z|$. This is signified by $\max \text{Im}(E) = 0$ regions that emerge at small γ when $h_z \neq 0$. (b) For edge sites, the $h_z = 0$ threshold at $\gamma/J = 0.25$, Eq.(5), is suppressed to vanishingly small values when $h_z = 0^+$ and increases with h_z thereafter (solid lines with symbols). For bulk sites, the threshold at $\gamma/J = 0.5$, Eq.(6), is also suppressed to zero for $h_z = 0^+$ and increases with h_z (dot-dashed lines).

the anti-diagonal, on the other hand, arises because the Hermitian term in Γ_p , Eq.(8), commutes with the Ising interaction term H_0 .

C. Effect of nonzero transverse field ($h_z \neq 0$)

When the transverse field h_z is introduced, the Hamiltonian H_{eff} contains three mutually non-commuting pieces, one for each Pauli matrix. Since the \mathcal{PT} -threshold results depend only on h_z , without loss of generality, we choose $h_z > 0$. First, we consider the fate of Hamiltonian Eq.(2) where potentials σ^\pm are introduced on sites p, q respectively. Apart from the trivial, Hermitian case ($p = q$), the behavior of the threshold γ_{PT} can be categorized as

$$\text{Adjacent sites: } \gamma_{\text{PT}}(h_z) = A_1 h_z, \quad (11)$$

$$\text{Both edge sites: } \gamma_{\text{PT}}(h_z) = (J/4) + A_2 h_z, \quad (12)$$

$$\text{One edge site: } \gamma_{\text{PT}}(h_z) = (J/4)\delta_{h,0} + A_3 h_z, \quad (13)$$

$$\text{Bulk sites: } \gamma_{\text{PT}}(h_z) = (J/2)\delta_{h,0} + A_4 h_z, \quad (14)$$

where A_k are configuration-dependent parameters. This behavior is also robust when the non-Hermitian perturbation is changed to

$$\Gamma'_{pq}(\gamma) \equiv \gamma(\sigma_p^+ + \sigma_q^+). \quad (15)$$

Figure 4 shows the typical dependence of $\max \text{Im}(E)(\gamma)$ on the transverse field h_z for Hamiltonian $H_{\text{eff}} = H_0 +$

Γ'_{pq} . For adjacent sites, $p = q \pm 1$, the zero threshold at $h_z = 0$ is lifted to values proportional to h_z . This is indicated by broadening of the region where $\max \text{Im}(E) = 0$ as γ is increased from zero (Fig. 4)(a). For non-adjacent cases, if one of the sites is at the edge, the $h_z = 0$ threshold is given by $\gamma_{\text{PT}} = J/4$. But it is suppressed to zero with the introduction of the transverse field. As h_z increases, the threshold also increases. Similar behavior is observed for $\max \text{Im}(E)(\gamma)$ when both sites are in the bulk (Fig. 4)(b)).

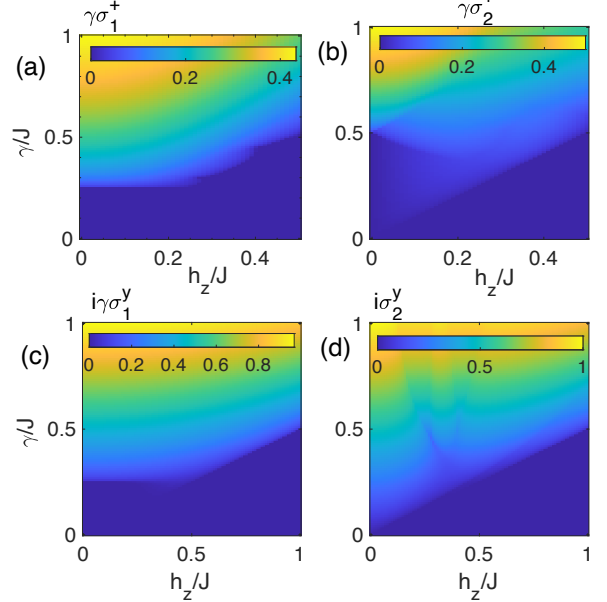


Figure 5. Evolution $\max \text{Im}(E)(\gamma, h_z)$ of the Hamiltonian Eq.(10) with $N = 7$ spins. Deep blue regions ($\max \text{Im}(E) = 0$) indicate \mathcal{PT} -symmetric phase. (a) For edge-site perturbation $\gamma\sigma_1^+$, the threshold increases from $J/4$ with increasing h_z . (b) For the same perturbation in the bulk, threshold increases from $\gamma_{\text{PT}}(h=0^+) = 0$ while its value is $J/2$ at $h_z = 0$. (c) same as (a) for anti-Hermitian, edge perturbation. (d) same as (b) for anti-Hermitian, bulk-site perturbation, where the no-field threshold is zero.

Lastly, we investigate h_z -dependence of γ_{PT} for the single-site perturbation model Eq.(10) by tracking the maximum imaginary part of its eigenvalues, $\max \text{Im}(E)(\gamma, h_z)$. Fig. 5(a) shows that for an edge-perturbation, starting from $J/4$ the threshold continuously increases with h_z . In contrast, when the exceptional potential $\gamma\sigma^+$ is on an interior site, the threshold $J/2$ at $h_z = 0$ is suppressed to vanishingly small values for $h_z \rightarrow 0$ before increasing linearly with h_z (Fig. 5(b)). When the edge-site potential is purely anti-Hermitian, starting from $J/4$, the threshold further increases continuously with h_z (Fig. 5(c)). Figure 5(d) shows that when the anti-Hermitian potential $i\gamma\sigma^y$ is in the bulk, the zero threshold at $h_z = 0$ is linearly lifted. Thus, the transverse field can strengthen or weaken the \mathcal{PT} -symmetric phase.

III. SYMMETRIES AND THE \mathcal{PT} -BREAKING THRESHOLD

The simple, N -independent results for the \mathcal{PT} -breaking threshold for a quantum Ising chain in the absence of a transverse field hint at an analytical solution. The robustness of that threshold γ_{PT} points to the possibility of investigating the interplay between the h_z/J -driven quantum phase transition and the γ/J -driven \mathcal{PT} symmetry breaking transition. Here, we discuss the analytical solution for $h_z = 0$.

Consider the zero-field model with a single-site perturbation $\Gamma_p(\gamma, 0)$, Eq.(8). The eigenstates of H_0 , Eq.(1), can be written as $|\psi\rangle = |\pm_1\rangle \otimes |\pm_2\rangle \cdots |\pm_N\rangle$ where $\sigma_m^x |\pm_m\rangle = \pm |\pm_m\rangle$ are the symmetric (anti-symmetric) eigenstates at site m . For a perturbation on site p , we consider an eigenstate ansatz as

$$|\phi\rangle \equiv |\pm_1\rangle \cdots |\hat{n}_p\rangle \cdots |\pm_N\rangle, \quad (16)$$

where $|\hat{n}_p\rangle$ denotes the spin state at the perturbation site. The eigenvalue equation satisfied by the state $|\phi\rangle$ becomes

$$H_p |\hat{n}_p\rangle = \left[h_x \sigma^x + i \frac{\gamma}{2} \sigma^y \right] |\hat{n}_p\rangle = E_p |\hat{n}_p\rangle, \quad (17)$$

$$h_x = -J \langle \phi | \sigma_{p-1}^x + \sigma_{p+1}^x | \phi \rangle + \frac{\gamma}{2} \sigma^x, \quad (18)$$

where one of the $p \pm 1$ terms is absent when the location p is at the edge. The 2×2 Hamiltonian H_p Eq.(17) undergoes \mathcal{PT} -symmetry breaking when the strength of the imaginary field is equal to that of the real field, i.e $h_x = \pm \gamma/2$. This gives Eq.(9) as the threshold result. A similar analysis can be carried out for other exceptional potentials, including two-site potentials, Eq.(3), when the two sites are not adjacent. When the two sites are adjacent, a similar reduction to a 4×4 Hamiltonian gives the zero threshold, Eq.(4).

Note that although the two-site perturbation was motivated by splitting a Hermitian term into two Jordan-normal-form terms, symmetries in the $h_z = 0$ case map $\sigma^+ \leftrightarrow \sigma^-$ under a local, unitary transformation on the site of the potential. This equivalence between the two potentials is another reminder that in systems with bounded eigenvalue spectrum, "gain" and "loss" are

not equivalent to raising and lowering operators. Additional unitary-equivalent terms such as $\gamma\sigma^+ \leftrightarrow -\gamma\sigma^+$ or $h_z \leftrightarrow -h_z$ were already taken into account when obtaining the \mathcal{PT} threshold results.

IV. DISCUSSION

In this paper, we have developed a new class of \mathcal{PT} -symmetric quantum Ising models with N spins, where the non-Hermitian potentials are confined to one or two sites and the \mathcal{PT} -breaking threshold is independent of $N > 2$. In most traditional models, the non-Hermiticity is introduced by changing model parameters from real to complex; that means the number of sites with non-Hermiticity is proportional to N . Such complex extensions retain desirable features of the underlying models such as translational invariance, Jordan-Wigner integrability, etc. However, since each non-Hermitian qubit potential requires successful post-selection, implementing non-Hermitian potential on every site would require both local addressability and an exponential-in- N suppressed success-probability for post-selection. Both are challenging barriers.

Our models show that introducing a single non-Hermitian qubit in a Hermitian, quantum Ising chain gives rise to γ_{PT} that can be varied with the transverse field. With full control required over only the non-Hermitian qubit, our models provide a pathway to investigate the interplay between interaction and non-Hermitian properties. Our results remain qualitatively unchanged when the Hermitian Hamiltonian is changed from a quantum Ising model to its integer-spin counterpart or Heisenberg model with or without anisotropies. The spin-1 case, for example, is made richer by the possibility of different exceptional perturbations such as $S^+ = (S^x + iS^y)/2$ and $S^{+2} \neq 0$. An exact diagonalization analysis is required to obtain the general threshold $\gamma_{\text{PT}}(J_{xx}, J_{yy}, J_{zz}; \mathbf{h})$ as a function of the multiple, possible non-Hermiticities, and its exhaustive characterization is an open problem.

ACKNOWLEDGMENTS

This work is supported by ONR Grant No. N00014-21-1-2630. We thank P. Durganandini and Kater Murch for discussions.

[1] C. M. Bender and S. Boettcher, Real spectra in non-hermitian hamiltonians having pt symmetry, *Physical Review Letters* **80**, 5243 (1998).

[2] C. M. Bender, D. C. Brody, and H. F. Jones, Complex extension of quantum mechanics, *Phys. Rev. Lett.* **89**, 270401 (2002).

[3] A. Mostafazadeh, Pseudo-hermiticity versus PT symmetry: The necessary condition for the reality of the spectrum of a non-hermitian hamiltonian, *Journal of Mathematical Physics* **43**, 205 (2002).

[4] A. Mostafazadeh, Exact PT-symmetry is equivalent to Hermiticity, *Journal of Physics A: Mathematical and*

General **36**, 7081 (2003).

[5] C. M. Bender, Making sense of non-hermitian hamiltonians, *Reports on Progress in Physics* **70**, 947 (2007), arXiv:hep-th/0703096.

[6] Y. N. Joglekar, C. Thompson, D. D. Scott, and G. Vemuri, Optical waveguide arrays: quantum effects and PT symmetry breaking, *The European Physical Journal Applied Physics* **63**, 30001 (2013).

[7] A. Guo, G. J. Salamo, D. Duchesne, R. Morandotti, M. Volatier-Ravat, V. Aimez, G. A. Siviloglou, and D. N. Christodoulides, Observation of \mathcal{PT} -symmetry breaking in complex optical potentials, *Phys. Rev. Lett.* **103**, 093902 (2009).

[8] C. E. Rüter, K. G. Makris, R. El-Ganainy, D. N. Christodoulides, M. Segev, and D. Kip, Observation of parity-time symmetry in optics, *Nature Physics* **6**, 192 (2010), 1003.4968.

[9] A. Regensburger, C. Bersch, M.-A. Miri, G. Onishchukov, D. N. Christodoulides, and U. Peschel, Parity-time synthetic photonic lattices, *Nature* **488**, 167 (2012).

[10] X. Zhu, H. Ramezani, C. Shi, J. Zhu, and X. Zhang, \mathcal{PT} -symmetric acoustics, *Phys. Rev. X* **4**, 031042 (2014).

[11] B. Peng, S. K. Özdemir, F. Lei, F. Monifi, M. Gianfreda, G. L. Long, S. Fan, F. Nori, C. M. Bender, and L. Yang, Parity-time-symmetric whispering-gallery microcavities, *Nature Physics* **10**, 394 (2014).

[12] H. Hodaei, M.-A. Miri, M. Heinrich, D. N. Christodoulides, and M. Khajavikhan, Parity-time-symmetric microring lasers, *Science* **346**, 975 (2014).

[13] J. Schindler, A. Li, M. C. Zheng, F. M. Ellis, and T. Kottos, Experimental study of active LRC circuits with PT symmetries, *Physical Review A - Atomic, Molecular, and Optical Physics* **84**, 1 (2011).

[14] C. M. Bender, B. K. Berntson, D. Parker, and E. Samuel, Observation of PT phase transition in a simple mechanical system, *American Journal of Physics* **81**, 173 (2013).

[15] Y. N. Joglekar, R. Marathe, P. Durganandini, and R. K. Pathak, PTspectroscopy of the rabi problem, *Physical Review A* **90**, 040101 (2014).

[16] M. Chitsazi, H. Li, F. Ellis, and T. Kottos, Experimental realization of floquet \mathcal{PT} -symmetric systems, *Physical Review Letters* **119**, 093901 (2017).

[17] M. A. Quiroz-Juárez, K. S. Agarwal, Z. A. Cochran, J. L. Aragón, Y. N. Joglekar, and R. d. J. León-Montiel, On-demand parity-time symmetry in a lone oscillator through complex synthetic gauge fields, *Phys. Rev. Appl.* **18**, 054034 (2022).

[18] Z. A. Cochran, A. Saxena, and Y. N. Joglekar, Parity-time symmetric systems with memory, *Phys. Rev. Research* **3**, 013135 (2021).

[19] A. Wilkey, G. Vemuri, and Y. N. Joglekar, Exceptional points in a time-delayed parity-time symmetric system, in *Active Photonic Platforms XII*, edited by G. S. Subramania and S. Foteinopoulou (SPIE, 2020).

[20] J. Zhang, L. Li, G. Wang, X. Feng, B.-O. Guan, and J. Yao, Parity-time symmetry in wavelength space within a single spatial resonator, *Nature Communications* **11**, 10.1038/s41467-020-16705-8 (2020).

[21] Q. Ding, M. Wang, J. Zhang, Y. Tang, Y. Li, M. Han, Y. Guo, N. Zhang, B. Wu, and F. Yan, Parity-time symmetry in parameter space of polarization, *APL Photonics* **6**, 076102 (2021).

[22] R. Kubo, The fluctuation-dissipation theorem, *Reports on Progress in Physics* **29**, 255 (1966).

[23] C. M. Caves, Quantum limits on noise in linear amplifiers, *Physical Review D* **26**, 1817 (1982).

[24] S. Scheel and A. Szameit, \mathcal{PT} -symmetric photonic quantum systems with gain and loss do not exist, *EPL (Europhysics Letters)* **122**, 34001 (2018).

[25] L. Xiao, X. Zhan, Z. H. Bian, K. K. Wang, X. Zhang, X. P. Wang, J. Li, K. Mochizuki, D. Kim, N. Kawakami, W. Yi, H. Obuse, B. C. Sanders, and P. Xue, Observation of topological edge states in parity-time-symmetric quantum walks, *Nature Physics* **13**, 1117 (2017).

[26] J. Li, A. K. Harter, J. Liu, L. de Melo, Y. N. Joglekar, and L. Luo, Observation of parity-time symmetry breaking transitions in a dissipative floquet system of ultracold atoms, *Nature Communications* **10**, 10.1038/s41467-019-08596-1 (2019).

[27] Y. Wu, W. Liu, J. Geng, X. Song, X. Ye, C.-K. Duan, X. Rong, and J. Du, Observation of parity-time symmetry breaking in a single-spin system, *Science* **364**, 878 (2019).

[28] N. Maraviglia, P. Yard, R. Wakefield, J. Carolan, C. Sparrow, L. Chakhmakhchyan, C. Harrold, T. Hashimoto, N. Matsuda, A. K. Harter, Y. N. Joglekar, and A. Laing, Photonic quantum simulations of coupled \mathcal{PT} -symmetric hamiltonians, *Phys. Rev. Res.* **4**, 013051 (2022).

[29] G. Lindblad, On the generators of quantum dynamical semigroups, *Comm. Math. Phys.* **48**, 119 (1976).

[30] V. Gorini, A. Kossakowski, and E. Sudarshan, Completely positive dynamical semigroups of n-level systems, *Journal of Mathematical Physics* **17**, 821 (1976).

[31] D. Manzano, A short introduction to the lindblad master equation, *AIP Advances* **10**, 025106 (2020).

[32] K. Mølmer, Y. Castin, and J. Dalibard, Monte carlo wave-function method in quantum optics, *Journal of the Optical Society of America B* **10**, 524 (1993).

[33] F. Minganti, A. Miranowicz, R. W. Chhajlany, and F. Nori, Quantum exceptional points of non-hermitian hamiltonians and liouvillians: The effects of quantum jumps, *Physical Review A* **100**, 062131 (2019).

[34] D. C. Brody and E.-M. Graefe, Mixed-state evolution in the presence of gain and loss, *Physical Review Letters* **109**, 230405 (2012).

[35] M. Naghiloo, M. Abbasi, Y. N. Joglekar, and K. W. Murch, Quantum state tomography across the exceptional point in a single dissipative qubit, *Nature Physics* **15**, 1232 (2019).

[36] F. Klauck, L. Teuber, M. Ornigotti, M. Heinrich, S. Scheel, and A. Szameit, Observation of PT-symmetric quantum interference, *Nature Photonics* **13**, 883 (2019).

[37] L. Ding, K. Shi, Q. Zhang, D. Shen, X. Zhang, and W. Zhang, Experimental determination of \mathcal{PT} -symmetric exceptional points in a single trapped ion, *Phys. Rev. Lett.* **126**, 083604 (2021).

[38] C. Korff, PTsymmetry of the non-hermitian XX spin-chain: non-local bulk interaction from complex boundary fields, *Journal of Physics A: Mathematical and Theoretical* **41**, 295206 (2008), arXiv:0803.4500 [math-ph].

[39] O. A. Castro-Alvaredo and A. Fring, A spin chain model with non-hermitian interaction: the ising quantum spin chain in an imaginary field, *Journal of Physics A: Mathematical and Theoretical* **42**, 465211 (2009).

[40] T. Deguchi and P. K. Ghosh, The exactly solvable quasi-

hermitian transverse ising model, *Journal of Physics A: Mathematical and Theoretical* **42**, 475208 (2009).

[41] X. Z. Zhang, L. Jin, and Z. Song, Dynamic magnetization in non-hermitian quantum spin systems, *Physical Review B* **101**, [10.1103/physrevb.101.224301](https://doi.org/10.1103/physrevb.101.224301) (2020).

[42] Y.-G. Liu, L. Xu, and Z. Li, Quantum phase transition in a non-hermitian XY spin chain with global complex transverse field, *Journal of Physics: Condensed Matter* **33**, 295401 (2021).

[43] L. Lenke, M. Mühlhauser, and K. P. Schmidt, High-order series expansion of non-hermitian quantum spin models, *Physical Review B* **104**, 195137 (2021).

[44] S. Bi, Y. He, and P. Li, Ring-frustrated non-hermitian XY model, *Physics Letters A* **395**, 127208 (2021).

[45] K. Yamamoto, M. Nakagawa, M. Tezuka, M. Ueda, and N. Kawakami, Universal properties of dissipative tomonaga-luttinger liquids: Case study of a non-hermitian xxz spin chain, *Phys. Rev. B* **105**, 205125 (2022).

[46] G. Chen, F. Song, and J. L. Lado, Topological spin excitations in non-hermitian spin chains with a generalized kernel polynomial algorithm, *Phys. Rev. Lett.* **130**, 100401 (2023).

[47] B. J. Ávila, C. Ventura-Velázquez, R. de J. León-Montiel, Y. N. Joglekar, and B. M. Rodríguez-Lara, \mathcal{PT} -symmetry from lindblad dynamics in a linearized optomechanical system, *Scientific Reports* **10**, [10.1038/s41598-020-58582-7](https://doi.org/10.1038/s41598-020-58582-7) (2020).

[48] C. H. Liang, D. D. Scott, and Y. N. Joglekar, \mathcal{PT} restoration via increased loss and gain in the \mathcal{PT} -symmetric aubry-andré model, *Physical Review A* **89**, [10.1103/physreva.89.030102](https://doi.org/10.1103/physreva.89.030102) (2014).

[49] E. Lieb, T. Schultz, and D. Mattis, Two soluble models of an antiferromagnetic chain, *Annals of Physics* **16**, 407 (1961).

[50] P. Pfeuty, The one-dimensional ising model with a transverse field, *Annals of Physics* **57**, 79 (1970).

[51] S. Sachdev, *Quantum Phase Transitions* (Cambridge University Press, 2009).

[52] E. Fradkin, *Field Theories of Condensed Matter Physics* (Cambridge University Press, 2013).

[53] F. Ruzicka, K. S. Agarwal, and Y. N. Joglekar, Conserved quantities, exceptional points, and antilinear symmetries in non-hermitian systems, *Journal of Physics: Conference Series* **2038**, 012021 (2021).